Biochemistry and Biophysics Reports 4 (2015) 169–174

Contents lists available at ScienceDirect

Biochemistry and Biophysics Reports

journal homepage: www.elsevier.com/locate/bbrep

Basal cells express functional TRPV4 channels in the mouse nasal epithelium

Takashi Ueda*, Mariko Hoshikawa, Yasuhiro Shibata, Natsuko Kumamoto, Shinya Ugawa

Department of Anatomy and Neuroscience, Graduate School of Medical Sciences, Nagoya City University, Nagoya, Japan

ARTICLE INFO

Article history:
Received 9 June 2015
Received in revised form
19 August 2015
Accepted 15 September 2015
Available online 16 September 2015

Keywords:
Transient receptor potential vanilloid type 4 (TRPV4)
Basal cells
Nasal epithelium
Immunohistochemistry
Calcium imaging
Mouse

ABSTRACT

Basal cells in the nasal epithelium (olfactory and airway epithelia) are stem/progenitor cells that are capable of dividing, renewing and differentiating into specialized cells. These stem cells can sense their biophysical microenvironment, but the underlying mechanism of this process remains unknown. Here, we demonstrate the prominent expression of the transient receptor potential vanilloid type 4 (TRPV4) channel, a Ca^{2+}-permeable channel that is known to act as a sensor for hypo-osmotic and mechanical stresses, in the basal cells of the mouse nasal epithelium. TRPV4 mRNA was expressed in the basal portions of the prenatal mouse nasal epithelium, and this expression continued into adult mice. The TRPV4 protein was also detected in the basal layers of the nasal epithelium in wild-type but not in TRPV4-knockout (TRPV4-KO) mice. The TRPV4-positive immunoreactions largely overlapped with those of keratin 14 (K14), a marker of basal cells, in the airway epithelium, and they partially overlapped with those of K14 in the olfactory epithelium. Ca^{2+} imaging analysis revealed that hypo-osmotic stimulation and 4α-phorbol 12,13 didecanoate (4α-PDD), both of which are TRPV4 agonists, caused an increase in the cytosolic Ca^{2+} concentration in a subset of primary epithelial cells cultured from the upper parts of the nasal epithelium of the wild-type mice. This response was barely noticeable in cells from similar parts of the epithelium in TRPV4-KO mice. Finally, there was no significant difference in BrdU-labeled proliferation between the olfactory epithelia of wild-type and TRPV4-KO mice under normal conditions. Thus, TRPV4 channels are functionally expressed in basal cells throughout the nasal epithelium and may act as sensors for the development and injury-induced regeneration of basal stem cells.

1. Introduction

The nasal epithelium is composed of olfactory (OE) and airway (respiratory) (AE) epithelia. The former (OE) is a simple, pseudostratified neuroepithelium that consists of olfactory receptor neurons (ORNs), glia-like supporting cells, globose basal cells (GBCs) and horizontal basal cells (HBCs). GBCs are a major proliferating cell population in the neuroepithelium and contain multipotent progenitors that generate neurons and supporting cells. HBCs, which are defined by their specific expression of keratin 5 (K5) and keratin 14 (K14), serve as a reservoir that replenishes GBC progenitors and (indirectly) neuronal and non-neuronal differentiated cells [1]. The AE is a simple, pseudostratified epithelium that consists of differentiated ciliated epithelial cells, mucous cells and basal cells. The basal cells have stemness/progenitor characteristics and play essential roles in epithelial remodeling [2]. Both the OE and AE have indirect contact with the external environment and many factors, including injury, mechanical stress, transcription factors and growth factors, regulate their neurogenesis and epithelial regeneration [3–9]. Thus, determining which receptors and sensors are expressed in these basal cells could contribute to the understanding of their function and regulation.

The transient receptor potential vanilloid type 4 (TRPV4) channel is a Ca^{2+}-permeable cation channel that can be activated by moderate temperatures (>25 °C), extracellular hypotonicity, shear stress, mechanical stress, the synthetic phorbol ester 4α-phorbol 12,13-didecanoate (4α-PDD), the botanical agent bisandrographolide A, and anandamide metabolites, including arachidonic acid (AA) [10–14]. It is expressed in some stratified epithelial cells, such as differentiated keratinocytes in skin [15] and undifferentiated basal cells in the urothelium [16] and esophageal epithelium [17,18]. Activation of this channel leads to an increase in the intracellular Ca^{2+} concentration ($[Ca^{2+}]_i$) and is involved in the regulation of a variety of Ca^{2+}-dependent cellular events, including proliferation [17] and differentiation. Therefore, TRPV4 receptors are likely candidates for the regulation of nasal epithelial functions. In the present study, we examined the expression and characteristics of TRPV4 channels in the mouse nasal epithelium using TRPV4-knockout (TRPV4-KO) mice.

* Correspondence to: Department of Anatomy and Neuroscience, Graduate School of Medical Sciences, Nagoya City University, 1 Kawasumi, Mizuho-cho, Mizuho-ku, Nagoya, Aichi 467-8601, Japan. Fax: +81 52 852 8887.
E-mail address: tueda@med.nagoya-cu.ac.jp (T. Ueda).

http://dx.doi.org/10.1016/j.bbrep.2015.09.008

2. Materials and methods

2.1. Animals

Adult male (8–10 weeks of age), neonatal (postnatal days 2 and 8; P2 and P8) and prenatal (embryonic day 18; E18) C57BL/6J mice were obtained from Japan SLC Inc. (Hamamatsu, Japan). TRPV4-KO mice (allele symbol *Trpv4*^{tm1Msz}) were kindly provided by Drs. Suzuki and Mizuno through the RIKEN BioResource Center (BRC) (RBRC01939), and their genotypes were determined by PCR as previously reported [19,20]. The mice were maintained under a 12-h light-dark cycle with sufficient water and food. All experimental protocols were approved by the Medical Animal Care Committee of Nagoya City University (permit number: H25M-05).

2.2. Reverse transcription PCR

Mouse RNA was isolated from the upper portions of the nasal mucosa in adult mice using Isogen (Wako Chemical, Osaka, Japan). Then, 3 μg of RNA were subjected to reverse transcription using random primers and SuperScript III (Invitrogen, Carlsbad, CA, USA). Next, 1/20 of the sample was amplified by PCR for 30 cycles with primer sets for carbonic anhydrase II [CAII (GenBank Accession No. NM_009801), 5′-gcattgtcaacaacggccact-3′ and 5′-ttctgaaggccttgtgaggca-3′ (position 500–800, yielding a 301 bp amplicon)] and TRPV4 and β-actin, as previously reported [18].

2.3. In situ hybridization

C57BL/6J mice at E18 were decapitated under deep anesthesia, and their heads were quickly frozen. Histological preparation of 16-μm sagittal sections and *in situ* hybridization were performed as previously described [21]. A [^{35}S]UTP-labeled complementary RNA probe for mouse TRPV4 (mTRPV4) was generated from nucleotide sequences 530-1726 (GenBank Accession No. NM_022017).

2.4. Immunohistochemistry

Fresh frozen coronal sections were obtained from P2 and P8 wild-type and TRPV4-KO mice using a cryostat. After the sections were air-dried, they were fixed with Bouin's fixative for 15 min at 4 °C and incubated with a rabbit anti-TRPV4 antibody (1:400) (Alomone Lab, Jerusalem, Israel) in phosphate-buffered saline (PBS) containing 5% normal donkey serum and 0.3% Triton X-100 overnight at 4 °C followed by an Alexa 594-conjugated donkey anti-rabbit IgG secondary antibody (Invitrogen). Specificity was confirmed by signal ablation in the TRPV4-KO mice. To confirm TRPV4 expression in basal cells, some fixed sections were reacted with rabbit anti-TRPV4 and guinea pig anti-keratin pan (PROGEN, Heidelberg, Germany) antibodies in PBS containing 5% normal goat serum and 0.3% Triton X-100 overnight at 4 °C, followed by incubation with Alexa 594-conjugated goat anti-rabbit IgG and Alexa 488-conjugated goat anti-guinea pig IgG secondary antibodies (Invitrogen).

2.5. Measurements of $[Ca^{2+}]_i$

The present calcium imaging analysis is based on previous experiments [17,18,22]. Briefly, single cell suspensions of epithelial cells from the upper portions of the nasal mucosa of adult wild-type and TRPV4-KO mice were obtained after enzymatic digestion with 0.05% trypsin for 20 min at 37 °C and fixed on coverglasses with Cell Tak medium. The fixed cells were incubated with the fluorescent Ca^{2+} indicator fura-2 acetoxymethyl ester (5 or 10 μM) (Invitrogen) for 30 min at room temperature. Changes in $[Ca^{2+}]_i$ in response to hypo-osmotic stimulation (228 mOm) and 4α-PDD (3 and 10 μM), both of which are TRPV4 activators, were recorded using an Olympus IX-70 microscope equipped with an ARGUS/HisCa system (Hamamatsu Photonics, Hamamatsu, Japan). As it was difficult to obtain a mean trace of basal cytosolic Ca^{2+} (controls) and a mean trace showing the effect of activators, we measured peak changes in the Ca^{2+} fluorescent ratio evoked by the TRPV4 activators (Δratio).

For the calcium image analysis, a standard 2-[4-(2-hydroxyethyl)-1-piperazinyl] ethanesulfonic acid (HEPES)-buffered solution with the following composition was used; NaCl 137, KCl 5.9, $CaCl_2$ 2.2, $MgCl_2$ 1.2, glucose 14, HEPES 10 (mM), pH 7.4 (pH 7.4 with NaOH). To apply the hypotonic solution, the cells were perfused with isotonic solution [NaCl 91.3, KCl 5.9, $CaCl_2$ 2.2, $MgCl_2$ 1.2, glucose 14, HEPES 10, mannitol 91 (mM), pH 7.4 (310 mOsm) (pH 7.4 with NaOH)] and then with hypotonic solution [NaCl 91.3, KCl 5.9, $CaCl_2$ 2.2, $MgCl_2$ 1.2, glucose 14, HEPES 10 (mM), pH 7.4 (228 mOsm) (pH 7.4 with NaOH)]. All experiments were performed at 25 ± 1 °C [22].

2.6. Bromodeoxyuridine (BrdU) labeling

Wild-type and TRPV4-KO mice at P8 were intraperitoneally injected with BrdU (Sigma; 250 μg) 30 min before they were sacrificed. Cryosections were fixed with 4% paraformaldehyde (PFA) in 0.1 M phosphate buffer for 30 min at 4 °C, incubated with 2 N HCl for 30 min at 37 °C, and then incubated with anti-mouse IgG Fab (1:200) (Jackson Immunoresearch, West Grove, PA, USA) for 2 h before immunostaining with an anti-BrdU antibody (mouse, 1:400; BD Biosciences, San Jose, CA, USA). An Alexa 488-conjugated donkey anti-mouse IgG F(ab')$_2$ secondary antibody (Jackson Immunoresearch) was used for visualization. Stained sections were viewed and photographed using a NIKON A1RSi confocal microscope (NIKON Corp., Tokyo, Japan). The mean number of immunoreactive cells ± standard error of the mean (SEM) was determined by counting the number of immunoreactive profiles using Image J software (NIH, MD, USA) (n=3 each, 10 fields of view in total).

3. Results

3.1. TRPV4 mRNA expression in mouse nasal epithelium

We isolated total RNA from the upper portions of adult mouse nasal epithelia and performed RT-PCR using a primer set specific for TRPV4. As shown in Fig. 1A, the TRPV4 transcript could be amplified from tissues that also contained transcripts encoding carbonic anhydrase II (CAII), which is expressed only in guanylyl cyclase-D (GC-D) neurons in the OE [23]. We also examined TRPV4 mRNA expression during different developmental stages using *in situ* hybridization with a [^{35}S]UTP-labeled riboprobe (Fig. 1B). Histochemical analysis results suggested that TRPV4 transcripts were already expressed in a subset of OE cells at E18 (Fig. 1B). Distinct silver grain accumulation (indicating positive labeling) was detected in the basal parts of the epithelium, as shown using an anti-sense probe, compared with the accumulation observed using the corresponding sense probe (Fig. 1B). The choroid plexus in the brain, which is known to express TRPV4 channels [10], was intensely labeled when only the anti-sense probe was used (Fig. 1B).

3.2. TRPV4 protein expression in mouse nasal epithelium

We performed immunostaining analysis using a rabbit polyclonal antibody against peptides mapping to a region near the C-terminus of the TRPV4 channel to confirm TRPV4 protein

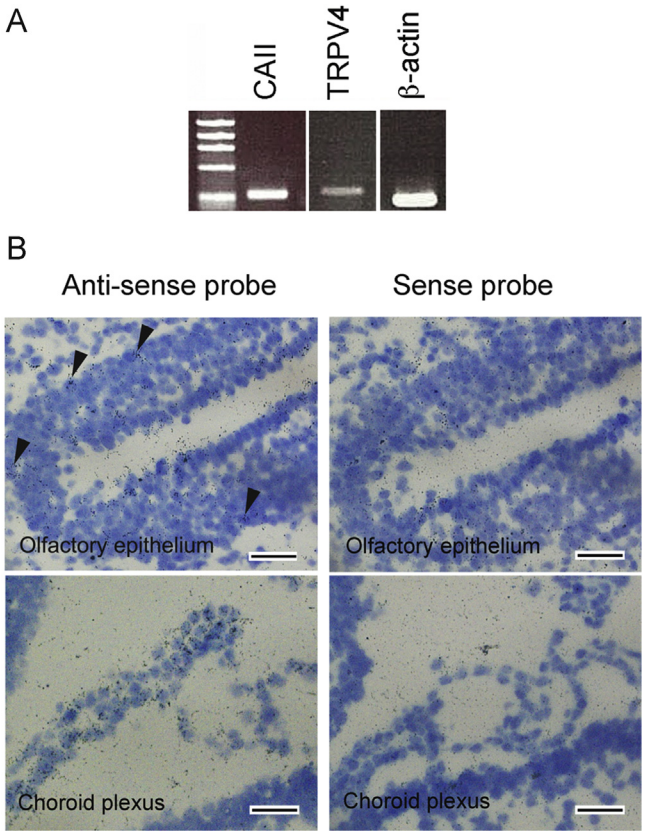

Fig. 1. (A) RT-PCR analysis of TRPV4 transcripts in adult mouse nasal mucosa. Controls, carbonic anhydrase II (CAII) and β-actin fragments are also shown. (B) Examination of the expression of TRPV4 transcripts in the mouse nasal mucosa at embryonic day 18 (E18) by *in situ* hybridization. Some cells located in the basal layer demonstrated intense TRPV4 expression when the TRPV4 anti-sense probe was used. Epithelial cells in the choroid plexus, which is known to express TRPV4 mRNA, also exhibited positive reactions when the anti-sense probe was employed. Scale bars: 30 μm.

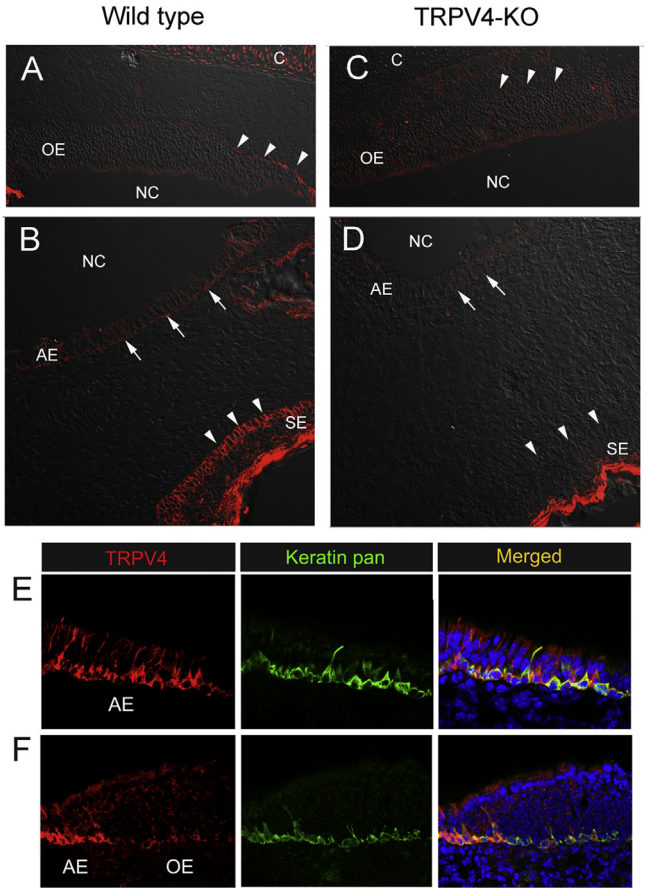

Fig. 2. Immunohistochemical analysis of TRPV4 in the mouse nasal mucosa. (A, B) Cellular localization of the TRPV4 protein in wild-type mice. TRPV4 was expressed in the basal layers of the olfactory epithelium (OE) (arrow heads) and the airway epithelium (AE) (arrows). TRPV4 immunoreactivity (IR) was also observed in the cartilage (C) and basal layers of the squamous epithelium (SE) (arrow heads in B). NC; nasal cavity (C, D). These structures were not stained in the TRPV4-KO mice (arrow heads and arrows). (E, F) Double-staining immunohistochemistry analysis of TRPV4 with keratin pan. TRPV4-IR is co-localized with keratin pan-positive (K14-positive) basal cells in the AE and OE.

expression in the mouse nasal epithelium. We have previously confirmed that this anti-TRPV4 antibody results in a prominent band approximately 100 kDa in size in total extracts from cultured HEK293T cells transfected with mTRPV4 cDNA but not in extracts from cells transfected with an empty vector [17,18]. As shown in Fig. 2A and B, the TRPV4 protein was detected mainly in the basal portion of both the OE and ciliated AE. This antibody also stained the cartilage (C) surrounding the nasal cavity (NC) and the basal layers of the squamous epithelium (SE) (Fig. 2A and B), in concordance with a previous study [12,18]. In contrast, no signals were detected in these structures in the TRPV4-KO mice (Fig. 2C and D), suggesting that the TRPV4 protein is predominantly expressed in the basal cells of the mouse nasal epithelium.

A previous report demonstrated that K5/K14-positive basal cells in the AE emerge before birth, in advance of HBCs in the OE. During the late prenatal stages in the mouse OE, HBCs are present only near the boundary with the AE, and the population of HBCs gradually expands and forms a basal layer throughout the OE by 2 weeks of age [24,25]. Thus, we determined which basal cell types express TRPV4 channels using coronal sections of mouse OE obtained during the late postnatal stage (P8). At this stage of development, most basal cells in the AE and OE were stained by anti-keratin pan antibody, which recognizes K14 (Fig. 2E and F). In addition, TRPV4 immunoreactivity (IR) was co-localized with that of K14-IR in most basal cells in the AE, whereas it overlapped with that of K14-IR only in a subset of HBCs near the boundary with the AE (Fig. 2E and F).

3.3. Functional TRPV4 expression in mouse nasal epithelium

To determine the functional expression of TRPV4 in the mouse nasal epithelium, we examined changes in $[Ca^{2+}]_i$ in response to a hypo-osmotic solution (228 mOsm) and 4α-PDD, both of which are TRPV4 agonists, using a Ca^{2+} imaging system and a Ca^{2+} fluorescent probe (fura-2/AM) in acutely dissociated epithelial cells from the upper portion of the nasal epithelium. The application of a hypo-osmotic solution (reducing the osmolarity from 310 to 228 mOsm) for 5 min caused an elevation of $[Ca^{2+}]_i$ in a subset of the total nasal epithelial cells examined. A subsequent longer application of ruthenium red (RuR), a non-selective antagonist of TRPV4 channels, suppressed the hypotonicty-induced activation in $9.1 \pm 0.5\%$ of the total nasal epithelial cells (average ± SEM, $n=5$ assays) (Δratio: 1.2 ± 0.02, average ± SEM, $n=17$ cells, $^{**}p < 0.0001$ vs. hypotonicity-insensitive cells, unpaired Student's *t* -test) (Fig. 3 A). Furthermore, the sequential application of 4α-PDD (5 and 10 μM) for 10 min also induced an increase in $[Ca^{2+}]_i$ and this response was markedly inhibited by 10 μM RuR in $10.0 \pm 2.3\%$ of the total nasal epithelial cells examined (average ± SEM, $n=3$ assays) (Δratio: 1.3 ± 0.04, average ± SEM, $n=10$ cells, $^{**}p < 0.0001$ vs. 4α-PDD-insensitive cells, unpaired Student's *t*-test) (Fig. 3B). We also examined the effect of a brief application of 10 μM 4α-PDD (90 s) to acutely dissociated nasal epithelial cells from wild-type and TRPV4-KO mice (Fig. 3C and D). A brief

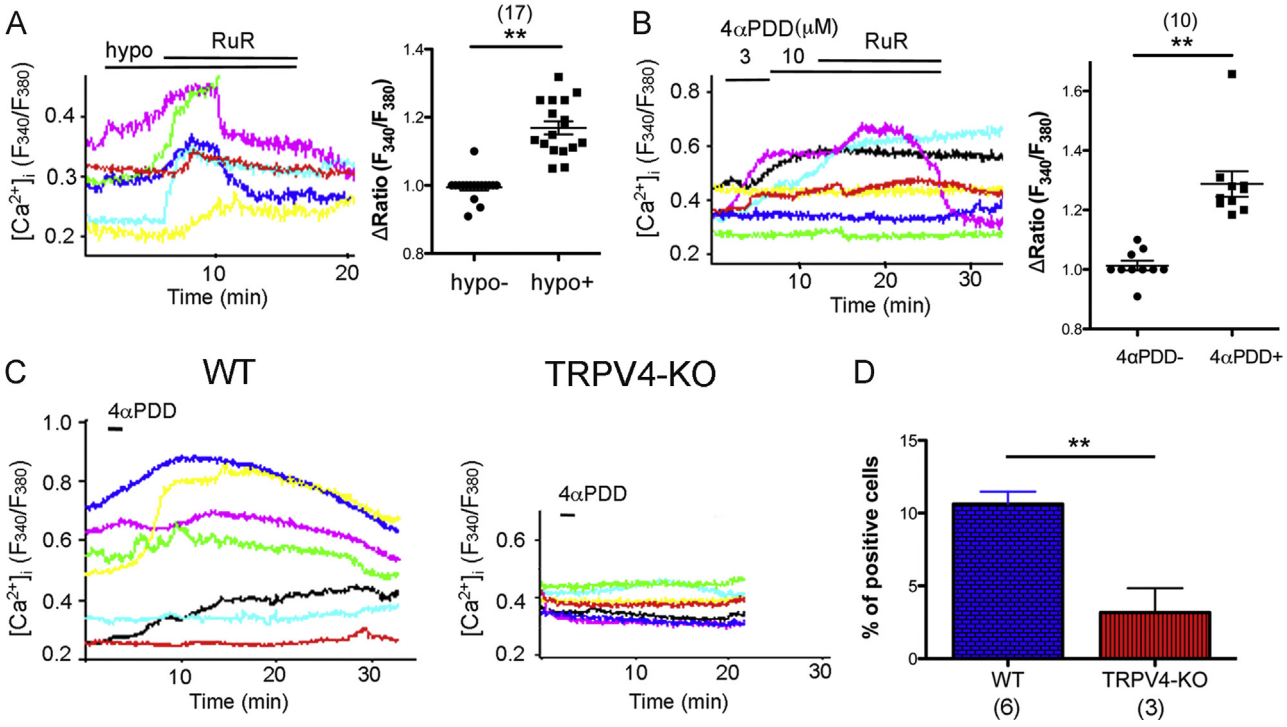

Fig. 3. Intracellular Ca^{2+} ($[Ca^{2+}]_i$) response in primary cultured mouse nasal epithelial cells. (A, B) Representative traces demonstrating that some cells responded to hypo-osmotic stimulation for 5 min (magenta and blue traces in A) and 4α-PDD for 10 min (magenta trace in B) and that the simultaneous application of ruthenium red (RuR) for 10–14 min suppressed the stimuli-induced Ca^{2+} increase (A and B) in wild-type mice. A summary of peak changes in the Ca^{2+} fluorescent ratio evoked by the TRPV4 activator (Δratio) is shown as a graph on the right in each panel. The number in parentheses indicates the number of cells analyzed. $^{**}p < 0.0001$ *vs.* stimulus-insensitive (hypo- or 4αPDD-) cells, unpaired Student's *t*-test). Bar=SEM. (C) Representative traces demonstrating that the brief application of 10 μM 4α-PDD (90 s) also caused an increase in $[Ca^{2+}]_i$ in a subset of the epithelial cells isolated from wild-type mice (yellow and black traces) (WT), whereas 4α-PDD-induced responses were rarely observed in cells obtained from TRPV4 KO mice (TRPV4-KO). (D) A significant difference between the results of wild-type (WT) and TRPV4-KO mice was observed ($^{**}p=0.0027$ *vs.* WT mice, unpaired Student's *t* -test). The number in parentheses under the bar graph indicates the number of assays performed. Bar=SEM.

application of 4α-PDD induced an increase in $[Ca^{2+}]_i$ in 10.7% of the total cells (58 of 543 total) in wild-type mice ($n=6$ assays, 12 animals). In the TRPV4-KO mice, in contrast, 4α-PDD-induced $[Ca^{2+}]_i$ transients were only observed in 3% of the total cells (8 of 237 total), a significant reduction ($^{**}p=0.0027$ vs. cells from wild-type mice, unpaired Student's *t*-test, $n=3$ assays, 6 animals) (Fig. 3C and D). Thus, a subpopulation of mouse nasal epithelial cells (approximately 10% of the total cell population) exhibited features of TRPV4-expressing cells.

3.4. BrdU incorporation in mouse OE

The finding of functional TRPV4 expression in basal cells suggests that the TRPV channel might affect the function and regulation of these progenitor cells, including their proliferation and differentiation. Moreover, there are two types of basal cells (GBC and HBC) in the OE. Thus, we examined the effect of TRPV4 on proliferation by BrdU labeling in P8 mice under normal conditions. Proliferating cells were labeled by intraperitoneal BrdU injection 30 min before the mice were sacrificed, and immuno-labeled cells in the OEs from the wild-type and TRPV4-KO mice were counted. However, no significant difference in BrdU labeling was observed between these two groups of mice (Fig. 4).

4. Discussion

The current study describes the isolation and characterization of TRPV4 in the mouse nasal epithelium. We concluded that TRPV4 channels were expressed in the basal cells of the nasal epithelium because TRPV4-IR in the epithelium was found to be primarily contained within K14-positive histological structures in our preparation, and responses to TRPV4-activators (hypotonic stress and 4α-PDD) were observed in a small subpopulation of acutely isolated nasal epithelial cells [approximately 10% of total nasal epithelial cells, which is an agreement with the basal cell population within the total nasal epithelial cell population (6–30% of total nasal epithelial cells [26])]. Interestingly, TRPV4-IR was detected in basal cells of both the OE and AE, but there were some differences between these epithelial types. TRPV4-IR was observed in almost all of the basal cells in the AE, whereas TRPV4-IR was selectively localized to K14-positive basal cells adjacent to the basement membrane in the OE. K14 is used as a specific maker for HBCs in the OE and K14-IR was indeed detected throughout the OE in P8 mice. In contrast, TRPV4 expression was restricted to a unique subpopulation of K14-positive HBCs that were only located near the boundary with the AE (the AE-OE boundary). HBCs are thought to emerge perinatally via two distinct patterns; a continuous population extending dorsalward from the AE-OE boundary and individual, scattered cells found throughout the OE [27]. Calcium signaling occurs in various cellular processes leading to cell migration. TRPV4 channels are also known to be involved in cell migration [28]. Thus, Ca^{2+}-permeable TRPV4 channels in HBCs that are located near the AE boundary may play a role in the migration of HBCs to the OE.

The physiological roles of TRPV4 channels in the basal cells of the nasal AE are currently unknown. Because TRPV4 is activated by a number of chemical and physical stimuli, including hypoosmotic, shearing and mechanical stresses, 4α-PDD and anandamide metabolites and leads to $[Ca^{2+}]_i$ mobilization, it could function as a polymodal sensor and play a role in stimulus-induced Ca^{2+}-dependent cellular events in the basal cells of the upper AE. In this context, we previously

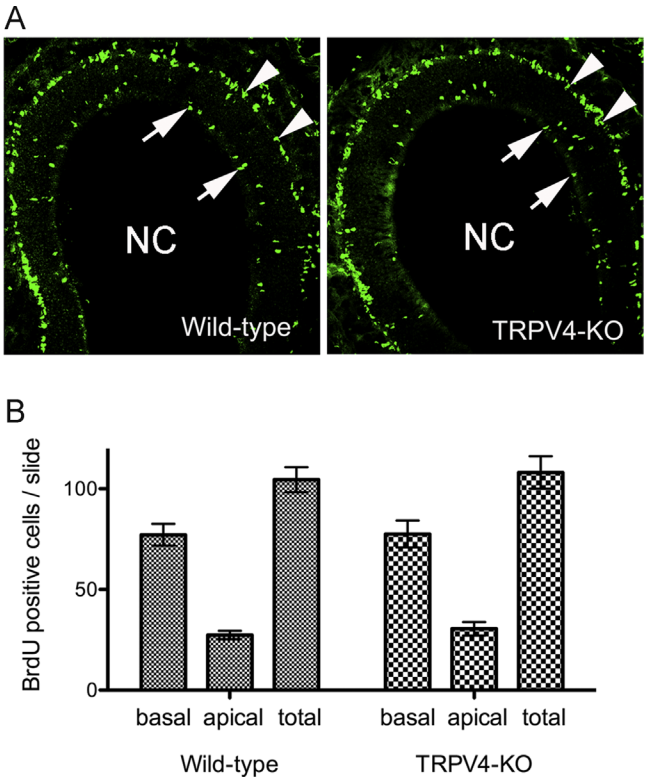

Fig. 4. *In vivo* BrdU proliferation assay in the olfactory epithelium (OE) of P8 mice. (A) Representative images of staining patterns with an anti-BrdU antibody in OEs isolated from wild-type and TRPV4-KO mice 30 min after an intraperitoneal BrdU injection. Note that BrdU-positive cells were observed in the apical (arrows) and basal (arrow heads) regions of the OEs in both wild-type and TRPV4-KO mice. NC; nasal cavity (B) BrdU-immunoreactive cells in the apical and basal portions of the OE, as shown in (A), were counted in 10 fields of view per animal, and each mean ± SEM is indicated ($n=3$ each). In the OE, there was no significant difference in BrdU labeling between wild-type and TRPV4 KO mice under normal developmental conditions.

demonstrated that the activation of TRPV4 affects cell viability and is linked to both cell proliferation and cell death in HET-1A human esophageal epithelial cells, which maintain characteristics of epithelial basal cells [17].

TRPV4 expression has been reported in the ciliated epithelial cells and vascular endothelial cells of the lower airway mucosa [29,30]. This protein participates in ciliary beat frequency regulation in mouse AE cells [29] and promotes acute, Ca^{2+}-dependent vascular permeability during pulmonary edema [30–32]. This study is the first report demonstrating TRPV4 channel expression in basal cells of the nasal epithelium. In the AE, basal cells are progenitor cells, and they can repopulate other cell types after injury in mice and humans [4,33]. Receptors for keratinocyte growth factor (KGF) [8] and epidermal growth factor (EGF) [9,34], which are involved in the repair of injured epithelia, are co-localized with a population of basal cells in the AE, but little is known about their regulation. In addition, these stem cells may contribute to epithelial immunity by secreting the antimicrobial protein RNase 7 in response to transient epithelial injury [35]. As our preliminary experiment showed no significant differences in BrdU-labeled proliferation between the P8 AEs of wild-type and TRPV4-KO mice under normal conditions, TRPV4 may act as a sensor for development and injury-induced epithelial remodeling in the upper AE.

Taken together, we found that the TRPV4 mRNA and protein were functionally expressed in a subset of HBCs in the OE and in basal cells of the AE. Thus, we speculate that TRPV4 may participate in a variety of cellular functions in basal cells, including immune responses and cell proliferation and regeneration. Interestingly, the expression of TRPV4 in basal cells has also been reported in other stratified epithelia, such as the urothelium [16] and esophageal epithelium [17], and TRPV4 may be a fundamental sensor molecule expressed in basal progenitor cells of epithelial tissues.

Acknowledgments

We thank Drs. Suzuki and Mizuno for providing the TRPV4-KO mice. This investigation was supported by a Grant-in-Aid for Scientific Research (C) from the Japan Society for the Promotion of Sciences (JSPS) KAKENHI (Grant number 24590281).

Appendix A. Supplementary material

Supplementary data associated with this article can be found in the online version at http://dx.doi.org/10.1016/j.bbrep.2015.09.008.

References

[1] C.T. Leung, P.A. Coulombe, R.R. Reed, Contribution of olfactory neural stem cells to tissue maintenance and regeneration, Nat. Neurosci. 10 (2007) 720–726.
[2] F. Yu, X. Zhao, C. Li, Y. Li, Y. Yan, L. Shi, B.R. Gordon, D.Y. Wang, Airway stem cells: review of potential impact on understanding of upper airway diseases, Laryngoscope 122 (2012) 1463–1469.
[3] V. Vedin, M. Molander, S. Bohm, A. Berghard, Regional differences in olfactory epithelial homeostasis in the adult mouse, J. Comp. Neurol. 513 (2009) 375–384.
[4] S.M. Warner, T.L. Hackett, F. Shaheen, T.S. HallstrandS, A. Kicic, S.M. Stick, D. A. Knight, Transcription factor p63 regulates key genes and wound repair in human airway epithelial basal cells, Am. J. Respir. Cell Mol. Biol. 49 (2013) 978–988.
[5] H. Nakamura, Y. Higuchi, H. Kondoh, M. Obata, S. Takahashi, The effect of basic fibroblast growth factor on the regeneration of guinea pig olfactory epithelium, Eur. Arch. Otorhinolaryngol. 259 (2002) 166–169.
[6] K. Isoyama, H. Nagata, Y. Shino, N. Isegawa, Y. Arimoto, M. Koda, K. Kumahara, Y. Okamoto, H. Shirasawa, Effects of adenoviral vector-mediated BDNF expression on the bulbectomy-induced apoptosis of olfactory receptor neurons, Brain Res. Mol. Brain Res. 129 (2004) 88–95.
[7] P. Barraud, X. He, C. Zhao, C. Ibanez, R. Raha-Chowdhury, M.A. Caldwell, R. J. Franklin, Contrasting effects of basic fibroblast growth factor and epidermal growth factor on mouse neonatal olfactory mucosa cells, Eur. J. Neurosci. 26 (2007) 3345–3357.
[8] W.L. Hicks Jr., L.A. Hall 3rd., R. Hard, J. Gardella, F. Bright, N. Parashurama, J. Lwebuga-Mukasa, L. Sigurdson, Keratinocyte growth factor and autocrine repair in airway epithelium, Arch. Otolaryngol. Head Neck Surg. 130 (2004) 446–449.
[9] N.T. Trinh, A. Privé, E. Maillé, J. Noël, E. Brochiero, EGF and K^+ channel activity control normal and cystic fibrosis bronchial epithelia repair, Am. J. Physiol. Lung Cell Mol. Physiol. 295 (2008) L866–L880.
[10] W. Liedtke, Y. Choe, M.A. Martí-Renom, A.M. Bell, C.S. Denis, A. Sali, A. J. Hudspeth, J.M. Friedman, S. Heller, Vanilloid receptor-related osmotically activated channel (VR-OAC), a candidate vertebrate osmoreceptor, Cell 103 (2000) 525–535.
[11] R. Strotmann, C. Harteneck, K. Nunnenmacher, G. Schultz, T.D. Plant, OTRPC4, a nonselective cation channel that confers sensitivity to extracellular osmolarity, Nat. Cell Biol. 2 (2000) 695–702.
[12] B. Nilius, G. Owsianik, T. Voets, J.A. Peters, Transient receptor potential cation channels in disease, Physiol. Rev. 87 (2007) 165–217.
[13] H. Watanabe, J.B. Davis, D. Smart, J.C. Jerman, G.D. Smith, P. Hayes, J. Vriens, W. Cairns, U. Wissenbach, J. Prenen, V. Flockerzi, G. Droogmans, C.D. Benham, B. Nilius, Activation of TRPV4 channels (hVRL-2/mTRP12) by phorbol derivatives, J. Biol. Chem. 277 (2002) 13569–13577.
[14] H. Watanabe, J. Vriens, J. Prenen, G. Droogmans, T. Voets, B. Nilius, Anandamide and arachidonic acid use epoxyeicosatrienoic acids to activate TRPV4 channels, Nature 424 (2003) 434–438.
[15] T. Sokabe, T. Fukumi-Tominaga, S. Yonemura, A. Mizuno, M. Tominaga, The TRPV4 channel contributes to intercellular junction formation in keratinocytes, J. Biol. Chem. 285 (2010) 18749–18758.
[16] T. Gevaert, J. Vriens, A. Segal, W. Everaerts, T. Roskams, K. Talavera, G. Owsianik, W. Liedtke, D. Daelemans, I. Dewachter, F. Van Leuven, T. Voets, D. De Ridder, B. Nilius, Deletion of the transient receptor potential cation channel TRPV4 impairs murine bladder voiding, J. Clin. Invest. 117 (2007)

3453–3462.
[17] T. Ueda, M. Shikano, T. Kamiya, T. Joh, S. Ugawa, The TRPV4 channel is a novel regulator of intracellular Ca^{2+} in human esophageal epithelial cells, Am. J. Physiol. Gastrointest. Liver Physiol. 301 (2011) G138–G147.
[18] M. Shikano, T. Ueda, T. Kamiya, Y. Ishida, T. Yamada, T. Mizushima, T. Shimura, T. Mizoshita, S. Tanida, H. Kataoka, S. Shimada, S. Ugawa, T. Joh, Acid inhibits TRPV4-mediated Ca^{2+} influx in mouse esophageal epithelial cells, Neurogastroenterol. Motil. 23 (2011) 1020–1028 , e497.
[19] M. Suzuki, A. Mizuno, K. Kodaira, M. Imai, Impaired pressure sensation in mice lacking TRPV4, J. Biol. Chem. 278 (2003) 22664–22668.
[20] A. Mizuno, N. Matsumoto, M. Imai, M. Suzuki, Impaired osmotic sensation in mice lacking TRPV4, Am. J. Physiol. Cell Physiol. 285 (2003) C96–101.
[21] T. Ueda, S. Ugawa, Y. Saishin, S. Shimada, Expression of receptor-activity modifying protein (RAMP) mRNAs in the mouse brain, Brain Res. Mol. Brain Res. 93 (2001) 36–45.
[22] N. Hatano, H. Suzuki, Y. Itoh, K. Muraki, TRPV4 partially participates in proliferation of human brain capillary endothelial cells, Life Sci. 92 (2013) 317–324.
[23] J. Hu, C. Zhong, C. Ding, Q. Chi, A. Walz, P. Mombaerts, H. Matsunami, M. Luo, Detection of near-atmospheric concentrations of CO_2 by an olfactory subsystem in the mouse, Science 317 (2007) 953–957.
[24] E.H. Holbrook, K.E. Szumowski, J.E. Schwob, An immunochemical, ultrastructural, and developmental characterization of the horizontal basal cells of rat olfactory epithelium, J. Comp. Neurol. 363 (1995) 129–146.
[25] A. Packard, N. Schnittke, R.A. Romano, S. Sinha, J.E. Schwob, DeltaNp63 regulates stem cell dynamics in the mammalian olfactory epithelium, J. Neurosci. 31 (2011) 8748–8759.
[26] J.R. Rock, S.H. Randell, B.L. Hogan, Airway basal stem cells: a perspective on their roles in epithelial homeostasis and remodeling, Dis. Model Mech. 3 (2010) 545–556 , Review.
[27] R.C. Krolewski, A. Packard, W. Jang, H. Wildner, J.E. Schwob, Ascl1 (Mash1) knockout perturbs differentiation of nonneuronal cells in olfactory epithelium, PLoS One 7 (2012) e51737.
[28] S. Mrkonjić, A. Garcia-Elias, C. Pardo-Pastor, E. Bazellières, X. Trepat, J. Vriens, D. Ghosh, T. Voets, R. Vicente, M.A. Valverde, TRPV4 participates in the establishment of trailing adhesions and directional persistence of migrating cells, Pflugers Arch. 467 (2015) 2107–2119.
[29] I.M. Lorenzo, W. Liedtke, M.J. Sanderson, M.A. Valverde, TRPV4 channel participates in receptor-operated calcium entry and ciliary beat frequency regulation in mouse airway epithelial cells, Proc. Natl. Acad. Sci. USA 105 (2008) 12611–12616.
[30] P.C. Villalta, M.I. Townsley, Transient receptor potential channels and regulation of lung endothelial permeability, Pulm. Circ. 3 (2013) 802–815.
[31] R.E. Morty, W.M. Kuebler, TRPV4: an exciting new target to promote alveolocapillary barrier function, Am. J. Physiol. Lung Cell Mol. Physiol. 307 (2014) L817–L821.
[32] N.M. Goldenberg, K. Ravindran, W.M. Kuebler, TRPV4: physiological role and therapeutic potential in respiratory diseases, Naunyn Schmiedebergs Arch. Pharmacol. 388 (2015) 421–436.
[33] R. Hajj, T. Baranek, R. Le Naour, P. Lesimple, E. Puchelle, C. Coraux, Basal cells of the human adult airway surface epithelium retain transit-amplifying cell properties, Stem Cells 25 (2007) 139–148.
[34] H.M. Brechbuhl, B. Li, R.W. Smith, S.D. Reynolds, Epidermal growth factor receptor activity is necessary for mouse basal cell proliferation, Am. J. Physiol. Lung Cell Mol. Physiol. 307 (2014) L800–L810.
[35] G.D. Amatngalim, Y. van Wijck, Y. de Mooij-Eijk, R.M. Verhoosel, J. Harder, A. N. Lekkerkerker, R.A. Janssen, P.S. Hiemstra, Basal cells contribute to innate immunity of the airway epithelium through production of the antimicrobial protein RNase 7, J. Immunol. 194 (2015) 3340–3350.